Influence of the latitudinal temperature gradient on soil dust concentration and deposition in Greenland

Ina Tegen[1]
Department of Applied Physics, Columbia University, New York

David Rind
NASA Goddard Institute for Space Studies, New York

Abstract

To investigate the effects of changes in the latitudinal temperature gradient and the global mean temperature on dust concentration in the Northern Hemisphere, experiments with the GISS GCM are performed. The dust concentration over Greenland is calculated from sources in central and eastern Asia, which are integrated on-line in the model. The results show that an increase in the latitudinal temperature gradient increases both the Asian dust source strength and the concentration over Greenland. The source increase is the result of increased surface winds, and to a minor extent, the increase in Greenland dust is also associated with increased northward transport. Cooling the climate in addition to this increased gradient leads to a decrease in precipitation scavenging, which helps produce a further (slight) increase in Greenland dust in this experiment. Reducing the latitudinal gradient reduces the surface wind and hence the dust source, with a subsequent reduction in Greenland dust concentrations. Warming the climate in addition to this reduced gradient leads to a further reduction in Greenland dust due to enhanced precipitation scavenging. These results can be used to evaluate the relationship of Greenland ice core temperature changes to changes in the latitudinal and global temperatures.

1. Introduction

Information about temperature conditions in the past can be obtained from stable isotope records from ice cores. However, those measurements represent only few points on the Earth. Ice cores are available from Greenland and Antarctica, with a few cores originating from lower latitudes, for example, the Dunde and Guliya ice caps in China [e.g., *Thompson et al.,* 1993] and the Quelccaya ice cap and Huascaran in Peru [e.g., *Thompson et al.,* 1994].

It is still not well understood to what extent temperature records from high latitudes and high altitudes represent the hemispherical temperature during different climate periods. A temperature decrease at high latitudes during glacial periods does not provide a unique assessment of hemispheric cooling; for example, it might represent an increase in the latitudinal temperature gradient, with tropical temperatures remaining largely unchanged, as in the Climate: Long-range Investigation, Mapping, and Prediction (CLIMAP) (1981) reconstruction for the Last Glacial Maximum (LGM). Another possibility is that a hemispheric (or global) cooling occurred, while the temperature gradient increased as well, as implied by stable isotope measurements from Huascaran in Peru [*Thompson et al.,* 1995*b*] and Guliya in China [*Thompson et al.,* 1997]. These results suggest that the tropical Atlantic and central Asia were cooler during the last glacial stage than at present (5°-6°C cooling was estimated for the tropical Atlantic), while at Greenland, the temperature decrease in the ice was estimated to be 15°C [*Cuffey and Clow,* 1997], up to 25°C [*Jouzel et al.,* 1997] colder than at present. As another example, it is unclear whether the cooler temperatures, which were observed especially in western Europe during the "Little Ice Age" (LIA) ($\approx$ 1500–1900 A.D.), were an indicator of a hemispherical cooling.

Usually, temperature decreases indicated by the stable isotope signals in polar regions are accompanied by an increase in the dust signal in ice cores. While *Mosley-Thompson et al.* [1993] reported no significant increase in the soil dust signal Greenland ice during the LIA, *O'Brien et al.* [1995] and *Mayewski et al.* [1993] show elevated dust in the GISP 2 core in Greenland during this period. Additionally, *Thompson et al.* [1993] find that most of the LIA period is characterized by elevated dust in the Guliya ice core (China).

During glacial periods, strong and rapid increases of dust concentration of more than an order of magnitude in both Greenland (e.g., GISP 2 and GRIP) and Antarctica (e.g., Vostok) are detected in ice cores [e.g., *Thompson and Mosley-Thompson,* 1981; *Mayewski et al.,* 1994; *Legrand,* 1995]. Various explanations for this strong increase have been suggested. Possible reasons for this dust signal include an increase in dust source areas due to decrease in vegetation cover or exposure of continental shelf [e.g., *Rea,* 1994], which may have served as a new dust source, an increase in surface wind speeds resulting in stronger dust deflation, or a more efficient transport from the source regions to the high latitudes by changes in the transport pathway or a reduction in dust deposition caused by a decrease in precipitation. Another possible cause for an increased dust flux might have been the increased availability of fine soil material deposited in glacial outwash, although the observed fast changes in the glacial dust signal point toward a change in atmospheric circulation as cause for this signal [*Biscaye et al.,* 1997].

Several attempts have been made to use a general circulation model (GCM) to explore the causes of this dust increase. GCMs that only consider changes in atmospheric conditions have been unable to simulate the strong dust increase of more than an order of magnitude in the Greenland dust during the LGM [*Joussaume,* 1993; *Genthon,* 1992]. Recently, *Andersen et al.* [1998] simulated the impact of exposed continental shelves (caused by sea level changes) on dust emissions and transport to Greenland in addition to changes in soil moisture and changes in wind and precipitation during LGM conditions. They obtained an increase in the Greenland dust deposition in their model by a factor of 2-3 during LGM conditions caused by this new dust source, mainly from a small source area that was simulated in northern Greenland. However, it is not clear how effective such exposed shelf areas may have been as dust sources, since they may have been covered by vegetation or ice. *Biscaye et al.* [1997] find strong evidence from the isotope measurements that Greenland dust originated from eastern Asia, while sources in midcontinental United States and Sahara for Greenland dust can be excluded as potential source areas. However, since there is a lack of samples at high latitudes such as Siberia or northern Greenland, these high-latitude source areas cannot be excluded as possible source regions for the dust found in the Greenland ice cores.

If we disregard changes in soil surface conditions, both the changes in the latitudinal temperature gra-

dient and the changes in the average temperature may cause a change in the dust signal in Greenland by changes in wind speeds, precipitation, or changes in circulation patterns. In an attempt to distinguish these alternatives, in this paper we investigate the consequences of such changes on dust concentrations at Greenland. This follows an investigation by *Rind* [1998], who evaluated the effects of a change in the latitudinal sea surface temperature (SST) gradient using the Goddard Institute for Space Studies (GISS) GCM. (Here we do not attempt to use a GCM to simulate all of the possible processes involved in creating the strong dust signal in Greenland, since many boundary conditions responsible for dust deflation during different climate periods like soil surface conditions are difficult to constrain.) If changes in dust transport to Greenland can be attributed to either changes in temperature gradient or changes in global average temperatures, we might be able to infer changes in the latitudinal temperature gradient from the observed Greenland dust records. This may give an additional indication whether the temperature gradient information we can obtain from the limited amount of ice records in the Northern Hemisphere (NH) is sufficient to reconstruct the hemispherical temperature conditions. This investigation is specifically of interest for time periods where land surface conditions, which could potentially affect dust deflation, did not change considerably (vegetation changes or addition of glacial outwash), since those changes were not included in the simulation.

2. Dust As Tracer in the GISS GCM

Dust has been included as a dynamic tracer in the GISS atmospheric GCM (4° × 5°horizontal resolution, nine vertical layers). This parameterization and some results thereof have been described by *Tegen and Miller* [1998]. Dust sources, transport, and deposition were computed with a 1-hour time step. In the GCM, dust emissions are computed as a function of vegetation cover, surface wind speed, and soil moisture [*Tegen and Fung,* 1994]. Dust deflation is allowed in areas labeled by *Matthews* [1983] as deserts or sparsely vegetated regions. The GCM transports four size classes of dust, with size ranges of 0.1-1, 1-2, 2-4, and 4-8 μm as independent tracers. Sizes below 1 μm were transported as one size class because they are not strongly fractionated by gravitational settling. Particle sizes larger than 8 μm were not included in this calculation, since large particles fall out quickly and are not important for long-range dust transport. Surface distributions of clay (particles smaller than 1 μm) and small silt (particle radius between 1 and 10 μm) were derived from a global soil texture data set [*Zobler,* 1986; *Webb et al.,* 1991]. Measurements show that above a critical threshold velocity (below which no dust deflation takes place), dust fluxes into the atmosphere depend on the third power of surface wind speed [*Gillette,* 1978] which is the most critical parameter for calculating dust emissions on the global scale. In the model the dust flux in those areas, where the surface conditions allow dust deflation, follows

$$q_a = C(u - u_{tr})u^2, \qquad (1)$$

where q_a is the dust flux from the surface in μg m^{-2} s^{-1}, u is the surface wind speed in m s^{-1}, and u_{tr} is a threshold velocity. For wind speeds below this threshold, no dust deflation takes place. We used the dimensional constant of $C = 2$ μg s^2 m^{-5} for clay particles (< 1 μm) and $C = 5$ μg s^2 m^{-5} for silt particles (1-8 μm) to describe dust deflation [*Tegen and Miller,* 1998]. Because the dust emissions increase nonlinearly with surface wind speed, peak wind speed events are responsible for a major part of dust deflation. High-wind events in the GCM are less frequent compared to the previously used European Centre for Medium-Range Weather Forecasts (ECMWF) surface-wind products with a spatial resolution of 1.125° × 1.125° [*Tegen and Fung,* 1994]. This leads to an underestimate of dust emissions in the GCM experiments. To reduce this difference, we chose a threshold velocity for each land grid box in the GCM that results in the same dust fluxes compared to the off-line model with ECMWF surface winds (for which the threshold velocity was 6.5 m s^{-1} at all locations) [*Tegen and Fung,* 1995]. The resulting threshold velocities for GCM surface wind speed vary between 4 and 10 m s^{-1}. We chose to vary the threshold velocities at each gridbox instead of varying the emission factor, because this way the number of dust events occurring per year at each gridbox would be similar to the off-line results that used the ECMWF surface wind product.

Dust is removed from the atmosphere by gravitational settling using Stokes law (size-dependent settling velocities), turbulent mixing in the first model layer, and subcloud washout calculated using GCM precipitation. A detailed description of this parameterization and the validation of the results under present-day conditions can be found in the work of *Tegen and Miller* [1998]. For these experiments, only Asian dust sources are included; that is, dust fluxes

from other continents are zero. We include only Asian sources, since *Biscaye et al.* [1997] deduce from a comparison of the clay mineralogy and isotope composition of dust from the GISP 2 ice core that dust arriving at Greenland originated most likely from eastern Asia. They ruled out sources in Sahara or the continental United States as contributors to Greenland dust. Since that study could not exclude all other possible source regions, it cannot prove conclusively that all Greenland dust originates only from Asian sources. However, this assumption is supported by a climatology of air mass trajectories arriving at Greenland [*Kahl et al.*, 1997].

The GISS GCM was integrated using different (fixed) SST distributions as boundary conditions. Each run was carried out for 11 model years, the results of the last 10 model years were averaged for the results shown in this paper. We carried out GCM integrations with changes only in the latitudinal gradient, while the global average temperature was kept at present-day level, and additional integrations in which the global average temperatures were changed additionally to the gradient changes. This allowed us to investigate the impact of temperature gradient change versus global mean temperature change separately. These SST boundary conditions correspond to the experiments described by *Rind* [1998].

The following GCM experiments were carried out:

A: The SST gradient between pole and equator was increased by 9°C; the global average temperature was kept at present-day levels.

B: The SST gradient between pole and equator was decreased by 9°C.

C: The SST gradient between pole and equator was increased by 9°C, and the average SST was decreased by 4°C.

D: The SST gradient between pole and equator was decreased by 9°C, and the average SST was increased by 4°C.

0: Present-day climatological SST control experiment.

3. Results and Discussion

We first show the results obtained for the dust distribution with present-day SSTs as boundary condition, before we show the results of the GCM integrations with changed SST conditions.

3.1. Control Experiment

Figure 1 shows the seasonal dust distribution of the first dynamic model layer that is obtained by using climatological averaged SSTs for present-day conditions (experiment 0). The source areas in central and east Asia are the Gobi and Taklimakan desert and the Kazakhstan region; these are potential source regions for dust transported to Greenland. Also, dust sources in the Sistan region in Iran as well as in Saudi Arabia [*Pye*, 1987] are predicted by the model; however, dust from these sources is not expected to contribute to dust in Greenland. The source areas predicted by the model agree well with areas where high dust storm frequencies are observed in Asia [e.g., *Littmann*, 1991]. The modeled dust production and eastward dust export from Asia peaks in the NH spring; this is in good agreement with many observations [e.g., *Gao et al.*, 1992]. *Tegen and Miller* [1998] show that the model realistically predicts concentrations of Asian dust transported over the North Pacific.

The seasonal cycle of the modeled dust concentration, deposition, and precipitation in Greenland is shown in Figure 2. The modeled summer maximum in the dust concentration and deposition does not agree with the spring maximum, which has been observed in the air and snow at Dye 3, Greenland [*Davidson et al.*, 1993; *Mosher et al.*, 1993], and with the maximum production of dust in Asia in spring. Since the GISP 2 site is at an elevation of 3300 m, it could be argued that the seasonal cycle of dust is rather reflected by the dust in GCM layer 3, which indicates the higher-altitude dust transport. In that layer, dust exhibits a higher early summer maximum compared to the dust seasonality of the first atmospheric layer. There, dust at Greenland is maximum in August/September as dust in the first model layer but has a stronger secondary maximum in May/June. However, since the spring peak of dust in Greenland is in April [*Davidson et al.*, 1993], regarding the dust transport in higher layers cannot explain the discrepancies in observed/modeled dust seasonalities at Greenland. This discrepancy may be due to two reasons: The summer maximum in Greenland dust modeled in the GCM may be influenced by dust from a minor northern Siberian source that is only active during the summer months (see Figure 1c). From this source region, dust is transported directly across the pole toward Greenland in the model. Compared to observations, the model slightly overestimates northward wind speeds in this region in NH summer, which may further enhance the modeled higher concentra-

tions of dust at Greenland in summer. No measurements (which we are aware of) exist to confirm or disprove the existence of a dust source in this high-latitude region. We do not know whether surface conditions in these regions actually allow for dust deflation.

Another explanation for this discrepancy between the observed and the modeled seasonal cycle of dust in Greenland could be that Saharan dust might occasionally be transported to Greenland. Even if clay and isotope measurements exclude the Sahara as a possible dust source area for Greenland dust during glacial periods, there are some indications from trajectory studies that during the NH spring, Saharan dust may be transported across Europe toward Greenland [*Mosher et al.*, 1993] at present times, and since this source is missing in these GCM experiments, the seasonal variation here may differ from the real world dust seasonality at Greenland. Particularly, this missing source may lead to an underestimate of dust in Greenland in NH spring. However, a 44-year climatology of air mass trajectories [*Kahl et al.*, 1997] does not include North Africa as a possible origin of air masses (and therefore Saharan dust) arriving at Greenland; and since *Biscaye et al.* [1997] find strong isotopic evidence that Greenland dust originated from Eastern Asia during the LGM and not from the Saharan desert, Saharan dust does not appear to be important for these calculations.

As shown in Table 1, the model control run produces dust concentrations at Greenland of 0.24 $\mu g/m^3$, which agrees reasonably well with the value of 0.4 $\mu g/m^3$ from measurements at Dye 3, Greenland (this value was derived from the arithmetic mean Fe concentration in Greenland aerosol cited in the reference, assuming a 3.5% Fe content of crustal aerosol).

Deposition rates at Greenland for the control run are 22 $mg/m^2/d$ (see Table 2), and the concentration of dust in the precipitation at Greenland is 160 $\mu g/kg$ water, which is more than a factor of 3 higher than the observed dust concentration of 46 $\mu g/kg$ in Greenland ice [*Steffensen*, 1997] for present-day conditions. Since the dust concentrations are modeled reasonably well, we assume that this discrepancy is due to an underestimate in precipitation in Greenland rather than an overestimate of dust transport. At the location of the GISP ice core (73°N, 39°W) the model produces a precipitation rate of 83 mm/yr, which is 3.5 times lower than the value given in the precipitation climatology by *Shea* [1986], who gives a value of 300 mm/yr at this location. The precipitation in the model also shows a maximum in summer at Greenland, which is in disagreement with the precipitation climatology by *Shea* [1986], which shows a fall/winter maximum at this location. Because of this discrepancy it is reasonable to focus the discussion of the GCM results on the dust concentrations at Greenland air rather than on the concentrations in the precipitation.

A comparison of dust concentrations in two ice cores, which were taken near the GISP site (sites A and T), is shown by *Mosher et al.* [1993]. Averaged over longer time periods, the dust concentrations are very consistent at those sites, but there are substantial year-to-year differences. Even at two cores at site T (which were drilled only 4 km apart) the year-to-year dust concentration can vary by as much as 50%. This illustrates the difficulty in comparing model results, which represent an average over 4° × 5°, with observations at a specific site.

3.2. Experiments A-D

Figure 3 shows the results for the annually and vertically averaged dust concentrations for the experiments A, B, C, D, and control experiment 0, together with the results for increased and decreased global SSTs only. The increased SST gradient (experiments A and C) results in an increase in dust concentrations, while the reduced gradient (experiments B and D) causes decreased dust concentrations compared to the control experiment. Table 1 shows the results for dust concentration at Greenland and dust source fluxes for the east and central Asian source regions for the different GCM experiments, together with the standard deviations (which are based on monthly averaged values). The results clearly show that the change in the temperature gradient is a major factor for increasing dust production in Asia and, as a consequence, the increase of dust transported to Greenland.

The increase in SST gradient (experiment A) leads to an overall increase in dust concentrations, with higher dust loads over the source regions in Asia as well as over Greenland. Table 1 shows that the dust concentration in Greenland is 2-3 times higher when the latitudinal temperature gradient is increased (experiment A) for averaged and first-layer dust concentrations compared to the control experiment 0. On the other hand, with a decreased latitudinal gradient (experiment B) the dust concentration (average and first layer) at Greenland decreases by about 20-50% compared to the control experiment (see Table 1). This decrease is smaller and less significant if com-

pared with the standard deviation than the increase in dust concentrations by the increase in the SST gradient. Figure 3 shows for case B similar concentrations near the source areas compared to the control case 0, but the concentrations over North America of dust transported eastward from Asia are smaller; that is, in this case, less dust is transported away from the source region. The response of dust concentrations to changes in the SST gradient is therefore not symmetrical, the sign of the change in the gradient does influence the strength in the dust response.

An additional decrease in global average SST together with the increased temperature gradient (experiment C) further increases the dust concentration at Greenland. However, the increase in the SST gradient (experiment A) increases the overall dust concentrations stronger compared to the control experiment than a decrease in global average SSTs alone. This becomes clear when considering the effect of SST decrease alone by subtracting the results of experiment C from experiment A (Figure 3, top middle panel). For this case, the concentration of dust above Asia is of the same order of magnitude as for the control case (experiment 0), but the dust is transported farther across North America. For experiment C the combination of these effects results in dust concentrations near the Asian source areas being similar to case A but also in slightly increased dust transport and concentration over North America and Greenland. There, the dust concentration in experiment C is $\approx$ 20% higher than for experiment A (see Table 1). This additional increase in Greenland dust is less significant than the increase of dust in experiment A compared to the control case, considering the large standard deviation.

For the opposite case, if the global mean temperatures are increased additionally to a decrease in latitudinal temperature gradient (experiment D), the dust concentration at Greenland is further reduced by about 30% compared to experiment B (Table 1). If only the effect of changes in global SST is considered compared to the change in the SST gradient only (by subtracting the results from experiment B from experiment D, middle panel in Figure 3), the dust concentrations over both Asian source areas and dust transport across North America are slightly reduced compared to the control experiment. For case D this change, together with the change due to the decrease in SST gradient, leads to a noticeable reduction of dust concentrations over the source areas and the dust transported eastward.

Because soil-surface conditions (e.g., changes in vegetation cover or land ice) did not change in these calculations, dust concentration changes can be caused by either changes in dust source strengths or changes in transport. Such changes, in turn, can be caused by changes in surface wind speed, changes in wind direction, or changes in precipitation, which can impact both washout rate of the dust during its transport and soil moisture in the source region, changing the source strength of dust.

3.3. Changes in Dust Source Strengths

Table 1 also summarizes the dust source strengths for the different GCM experiments. For increased SST gradients the source strength for eastern Asian (China) sources is increased by a factor of 3 compared to the control experiment, while the central Asian source is increased by a factor of $\approx$ 2. This corresponds well to the factor 2-3 increase in dust concentrations over Greenland for this case. On the other hand, a decrease in the SST gradient (case B) does not lead to a significant decrease in dust source strengths in Asia, as would have been expected if the response of the dust to the SST gradient change had been symmetrical.

For experiment C the eastern and central Asian source strengths of dust do not increase with an additional decrease in global mean SSTs, in fact, they are slightly lower than for experiment A. This indicates that for an increased gradient the increase in dustiness at Greenland is controlled by changes in the dust source strength, assuming the transport path is the same as in the control experiment. With additional colder temperatures the additional increase in Greenland dust must be caused by changes in transport or dust deposition. For the opposite case, an increase in global SSTs in addition to a decreased SST gradient (case D) leads to an $\approx$ 30% decrease in central Asian dust sources compared to case B (increased SST gradient only), while the Chinese dust sources remain effectively unchanged. This decrease is small compared to the standard deviation, however.

This change in dust source strength can be caused by changes in surface wind speed, which influences the dust deflation, or by changes in precipitation and soil moisture, which determines whether a given gridbox can act as a dust source (if the vegetation cover allows for dust deflation). Plates 1a-i show difference maps for the dust source strengths, surface wind speed, and precipitation for experiment A minus experiment B (the difference between the experiments

with increased and decreased SST gradients), experiment C minus experiment A (the effect of reducing the global SSTs but not changing the temperature gradients), and experiment D minus experiment B (the effect of increasing the global SSTs but not changing the temperature gradients). Plate 1a shows a strong increase in the dust source strengths with the change in SST gradients at all source locations. With a cooler climate (Plate 1b) the differences in dust sources are actually negative at most Asian source regions. For a warmer climate (Plate 1c) the eastern source regions increase, while the central Asian sources decrease.

Rind [1998] noted that the increase in latitudinal temperature gradient leads to an increase in zonal kinetic energy, which is consistent with an increase in surface winds. Plates 1d-1f show the difference in zonal wind speeds for the same differences as for Plates 1a-1c. The significant increase in westerly surface winds in midlatitude Asia for the increased compared to the decreased temperature gradient (Plate 1d) leads to increased dust deflation, since the dust flux depends, to the third power, on the surface wind speed. It should be noted that the monthly average wind speed itself is a less significant indicator for dust uplift than peak wind events in the source region due to the nonlinear dependency of dust deflation on the wind speed. Therefore areas of increased dust source strength are not necessarily closely correlated with areas of increase in mean wind speed.

For colder or warmer conditions without change in the latitudinal temperature gradient (Plates 1e and 1f), no significant change in surface wind speed occurs in the dust source areas. This corresponds to the result that the additional changes in source strengths for the experiments with decreased or increased SST in addition to increased or decreased latitudinal SST gradient are small. The latitudinal wind does not change significantly in any of the experiments with changed SST boundary conditions compared to the control experiment.

Plates 1g-1i show precipitation differences for the same cases as Plates 1a-1c. Changes in precipitation can potentially influence dust sources by changing soil moisture, and on the other hand, they can change transport efficiency by changing washout rates. First, we evaluate changes in precipitation over Asia in response to SST changes, to determine the possible impact on dust source strengths. The change of the latitudinal temperature gradient alone does not influence the precipitation in the Asian dust source area (Plate 1g), the same holds true for the colder climate (Plate 1h). Warming the climate leads to an increase in precipitation in the source area (Plate 1i), especially for eastern Asian sources. However, this precipitation change alone does not control soil moisture in the source area, since the evaporation from the soil is also changed with the changed global temperatures. The increase in global SSTs by 4°C (experiment D) results actually in a decrease in soil moisture in the source area by 20% due to increased evaporation, while experiment C (decreased temperatures) results in slightly higher soil moistures by 5% compared to the control experiment. The change in latitudinal temperature gradient alone (experiments A and B) does not influence the soil moisture in the Asian dust source region. This soil moisture change could explain the slight decrease in dust flux in experiment C compared to experiment A (see Table 1), and the slight dust flux decrease in the eastern Asian sources in experiment D compared to experiment C. The effect of a decreasing soil moisture in the warmer climate on dust source fluxes is small, however, since soil moisture influences the dust flux only as a threshold variable. We would expect changes in soil moisture to influence vegetation cover, such changes were not included in the model and cannot be discussed here.

3.4. Changes in Dust Transport

The dust transport itself is influenced by changes in precipitation, since a decrease in precipitation would lead to a decrease in dust washout, which would allow the dust to be transported farther from the Asian source area across the North American continent toward Greenland. Plates 1g-1i show that in the Northern Hemisphere the precipitation changes regionally with changes in latitudinal temperature gradient (Plate 1g), while the colder climate (Plate 1h) leads to lower precipitation and the warmer climate to higher precipitation (Plate 1i) over the entire NH. For changes in the latitudinal gradient only (Plate 1g), the average precipitation north of 30°N (where the precipitation can affect the dust transport to Greenland) slightly decreases in experiment A by 4% and increases in experiment B by 7%, respectively. These changes are small, compared to the changes in dust source strengths, and have presumably little effect on the dust concentrations at Greenland. The average of the NH precipitation north of 30°N shows a decrease for experiment C by 26% compared to the control experiment and an increase by 37% for experiment D compared to the control case. These changes in precipitation can explain the differences in the modeled

dust concentrations found in Greenland for the GCM integrations with changed average SSTs compared to changed latitudinal temperature gradients (Table 1), while differences in the dust source strengths cannot explain this difference (comparison of experiments A and C).

Dust transport may be affected not only by changes in the removal rates but also by changes in transport pathways. Northward dust transports for experiments A - D and control experiment 0 are shown in Figure 4 for the zonal mean. To compare the differences in the transport without including the changes in dust source strength and removal rates, the values for northward dust transport were divided by the total dust content of the atmosphere for each experiment. The northward transport of dust does not considerably change for the different SST boundary conditions. For experiment A (increased SST gradient) the northward dust transport between $\approx 40°$ and 70°N increases compared to the control experiment, for experiment C (additional cooling) there is only a small increase in northward dust transport compared to the control experiment. The changes in Greenland dust concentrations in the other experiments can therefore be explained by changes in source strengths due to changes in zonal wind speed and by changes in washout rates due to changes in precipitation strengths alone. For the increased temperature gradient (without changes in the global mean SST) an increase in northward transport also may be a factor causing the increased dust in Greenland. However, since for this case the factor of increase in Greenland dust concentrations agrees well with the factor of increase in dust source strength (see Table 1), we conclude that the changes in dust transport pathways are of comparatively minor importance.

3.5. Changes in Dust Deposition

The deposition of dust at Greenland is of interest, since the dust signal in ice cores reflects changes in the deposited dust on the ground rather than airborne dust concentrations at the ice core site. However, as mentioned above, the model underestimates the precipitation at Greenland and therefore overestimates dust concentrations in precipitation and may underestimate dust deposition fluxes at this location. Table 2 shows total and wet dust deposition at the GISP site for the GCM experiments together with the annual precipitation and annual mean dust concentration in precipitation (based on monthly averages). The wet deposition at this site is only about 50% of the total (wet plus dry) deposition for cases A and C, 60% for the control experiment, and $\approx$ 70% for cases B and D. This reflects the differences in precipitation in the model, which is by a factor of 2 smaller for the colder climate (experiment C), and by a factor of 2 higher for the warmer climate (experiment D) compared to the control experiment: for higher precipitation rates the wet deposition dominates the dry deposition at this remote location. Generally, dust deposition for the different GCM experiments follows the trend for dust concentrations, where the increase in SST gradient (experiment A) leads to an increase by a factor of $\approx$ 2-2.5 in the dust deposition (and concentration in precipitation), while the deposition flux for experiment C is not significantly higher than for case A. On the other hand, the dust concentration in precipitation is 30% higher for case C, which is due to the differences in the precipitation. The experiments with the decreased SST gradient also show a similar trend for deposition fluxes as the dust concentrations at Greenland, with the total deposition fluxes being about a factor of 2 smaller compared to the control run. These results indicate that even with the differences in precipitation at the Greenland location, the changes in deposition fluxes are similar to the changes in dust concentrations at this location.

3.6. Spring Conditions

As mentioned above, the dust signal at Greenland in the GCM shows a summer maximum, although the Asian dust source has a spring maximum. This discrepancy may be due to a high-latitude source that is active in the NH summer. Even though Asian sources north of 50°N contribute less than 10% and sources north of 60°N contribute less than 1% to the total Asian dust emission, such sources may disproportionally influence dust concentrations in Greenland. No measurements exist to prove or disprove the existence of a dust source at those high-latitude locations. Because of lack of measurements the existence of such a dust source cannot be excluded.

To evaluate whether the results presented here are still valid for the case that the model did incorrectly predict the existence of such a high-latitude Asian source, we investigated the GCM results for NH spring additionally to the annual averages. During NH spring the high-latitude Siberian source is not active, while dust emissions in Asia are largest. Table 3 summarizes the results for the Asian dust sources and Greenland dust concentration for NH spring. For case A, the increase in springtime dust concentration

is even higher than for the annual mean, with an increase by a factor of 4 for first layer dust concentrations and a factor of 2.4 increase for vertically averaged dust concentrations. This increase agrees with the 2.4-fold increase in dust source strengths for the combined Asian dust source regions in NH spring. On the other hand, for the reduced SST gradient (case B) the dust concentrations are reduced by 30-40% compared to the control experiment, corresponding to a 40% decrease in dust source strengths. Compared to the case of increased SST gradient, the additional cooling for case C leads to significantly lower dust concentrations at Greenland and dust source fluxes in Asia. This can be explained by changes in soil moisture: for NH spring, the soil water content in the dust source area is 21% higher in the model than in the control case, compared to the only 5% higher soil moisture in the dust source area in the annual mean for experiment C. This increase in soil moisture (caused by decrease in evaporation for the colder case) leads to a decrease in the available dust source area. As for the annual mean, the NH spring dust concentration at Greenland is lower for additional warming (D) compared to the decreased SST gradient only. This is due to the increase in washout during transport from the Asian source areas by increased precipitation.

Overall, the response in Greenland dust concentration in NH spring agrees with the response of the annual mean dust concentrations. Therefore we conclude that the results presented here are valid regardless of the existence of a high-latitude dust source which may impact dust concentrations at Greenland.

4. Conclusion

We estimated the effect of changes in the latitudinal temperature gradient and changes of the average global SST on the dust transport from Asia to Greenland. A significant 2-3-fold increase in dust load at Greenland can be found for increased temperature gradients. This can be explained by an increased source strength of dust in Asia, caused by an increase in surface wind speed and by increased northward transport. Precipitation in the source area and the area between the sources and Greenland did not change considerably. An additional decrease in global average SSTs does not additionally increase the dust source strength in Asia, however because of decreased washout due to decreased precipitation, the dust concentration at Greenland shows an additional increase for this case. On the other hand, for decreased latitudinal gradients the dust source strengths decrease, and an additional warming causes increased dust washout due to increased precipitation, therefore decreased dust concentrations (and deposition) at Greenland.

We can compare these results to observations of dust in Greenland. The model experiments most closely resemble the potential climate changes during the Little Ice Age (LIA), when land ice changes were not extensive. Isotopic observations imply colder conditions in Greenland from about 1500 to 1900. The dust record from the Dunde ice core in China (which may be influenced by local sources) does not show an obvious LIA response *Mosley-Thompson et al.* [1993]. On the other hand, *Thompson et al.* [1995*a*] find for the dust record in the Guliya ice core that most of the LIA period is characterized by elevated dust concentrations, which is also consistent with the historical dust fall records of *Zhang* [1984]. Also, *O'Brien et al.* [1995] and *Mayewski et al.* [1993] show from evidence in the GISP 2 core that dust concentrations in Greenland were elevated during later parts of the LIA. The model results would imply that there was a change in the latitudinal temperature gradient at the times of elevated dust. Isotopic evidence indicates cooling in the tropics (at Quelccaya, Peru) during the early part of the LIA, when dust levels were probably not increased. This could indicate a colder climate without any change in gradient, which according to the model results actually causes in a slightly decreased China source (Table 1).

Surface wind speeds increase because of the increased latitudinal temperature gradient in other major dust source regions, such as the Sahara, central North America, and central Australia. This could imply a similar relationship between dust deflation and temperature gradient. In that case, these results could be applied to the general increase in dust in Antarctica at this time which does imply an increased Southern Hemispheric latitudinal gradient as well as potentially cooler conditions. However, further GCM experiments are required before we are able to generalize these results. Observations of both isotopes and dust in ice core regions can be used to assess what the local temperature changes imply about changes in the latitudinal gradient and global mean temperatures.

The model results are less applicable for the Last Glacial Maximum (LGM), a time period with substantial increases of dust in Greenland. The increased temperature gradient at that time would have con-

tributed to greater dust concentrations, although gradient changes of the values given here were not sufficient to produce the order of magnitude increase found in the GISP ice core. Other obvious differences that were not taken into account in these calculations could explain these differences: changes in surface conditions (glacial outwash and vegetation decrease) would be expected to fundamentally increase the dust source strengths in Asia and subsequent transport to Greenland. Furthermore, the existence of large land ice sheets in the Northern Hemisphere could well have altered circulation patterns. Only a specific simulation with these boundary condition changes can act to provide a full assessment of the magnitude of the latitudinal gradient change applicable to the LGM.

Acknowledgments. This work was supported by the National Oceanic and Atmospheric Administration (NOAA grant NA56GP0450). We thank Dr. M. Prentice and an anonymous reviewer for useful discussions.

References

Andersen, K. K., A. Armengaud, and C. Genthon, Atmospheric dust under glacial and interglacial conditions, *Geophys. Res. Lett.*, *25*, 2281–2284, 1998.

Biscaye, P. E., F. E. Grousset, M. Revel, S. Van der-Gaast, G. A. Zielinski, A. Vaara, and G. Kukla, Asian provenance of glacial dust (stage 2) in the Greenland Ice Sheet Project 2 Ice Core, Summit, Greenland, *J. Geophys. Res.*, *102*, 26,765–26,781, 1997.

Cuffey, K. M., and D. G. Clow, Temperature, accumulation, and ice sheet elevation in central Greenland through the last deglacial transition, *J. Geophys. Res.*, *102*, 26,383–26,396, 1997.

Davidson, C. I., et al., Chemical constituents in the air and snow at Dye 3, Greenland I, Seasonal variations, *Atmos. Environ.*, *27*A, 2709–2722, 1993.

Gao, Y., R. Arimoto, J. T. Merril, and R. A. Duce, Relationships between the dust concentrations over eastern Asia and the remote North Pacific, *J. Geophys. Res.*, *97*, 9867–9872, 1992.

Genthon, C., Simulations of the long-range transport of desert dust and sea salt in a general circulation model, in *Precipitation Scavenging and Atmosphere-Surface Exchange*, edited by S. E. Schwartz and W. G. N. Slinn, pp. 1783–1794, Hemisphere Publ., Washington, D.C., 1992.

Gillette, D., A wind tunnel simulation of the erosion of soil: Effect of soil texture, sandblasting, wind speed, and soil consolidation on dust production, *Atmos. Environ.*, *12*, 1735–1743, 1978.

Joussaume, S., Paleoclimate tracers: An investigation using an atmospheric general circulation model under ice age conditions, 1, Desert dust, *J. Geophys. Res.*, *98*, 2767–2805, 1993.

Jouzel, J., et al., Validity of the temperature reconstruction from water isotopes in ice cores, *J. Geophys. Res.*, *102*, 26,471–26,487, 1997.

Kahl, J. D., A. M. Dewayne, H. Kuhns, C. I. Davidson, J. Jaffrezo, and J. M. Harris, Air mass trajectories to Summit, Greenland: A 44-year climatology and some episodic events, *J. Geophys. Res.*, *102*, 26,861–26,875, 1997.

Legrand, M., Atmospheric chemistry changes versus past climate inferred from polar ice cores, in *Aerosol Forcing of Climate*, edited by R. Charlson and J. Heintzenberg, pp. 123–152, John Wiley, New York, 1995.

Littmann, T., Dust storm frequency in Asia: Climatic control and variability, *Int. J. Climatol.*, *11*, 393–412, 1991.

Matthews, E., Global vegetation and land use: New high-resolution databases for climate studies, *J. Clim. Appl. Meteorol.*, *22*, 474–487, 1983.

Mayewski, P. A., L. D. Meeker, M. C. Morrison, M. S. Twickler, S. Whitlow, K. K. Ferland, D. A. Meese, M. R. Legrand, and J. P. Steffensen, Greenland ice core "signal" characteristics: An expanded view of climate change, *J. Geophys. Res.*, *98*, 12,839–12,847, 1993.

Mayewski, P. A., et al., Changes in atmospheric circulation and ocean ice cover over the North Atlantic during the last 41,000 years, *Science*, *263*, 1747–1751, 1994.

Mosher, B. W., P. Winkler, and J. L. Jaffrezo, Seasonal aerosol chemistry at Dye 3, Greenland, *Atmos. Environ.*, *27*A, 2761–2772, 1993.

Mosley-Thompson, E., L. G. Thompson, J. Dai, M. Davis, and P. N. Lin, Climate of the last 500 years: High resolution ice core records, *Quat. Sci. Rev.*, *12*, 419–430, 1993.

O'Brien, S. R., P. A. Mayewski, L. D. Meeker, D. A. Meese, M. S. Twickler, and S. I. Whitlow, Complexity of Holocene climate as reconstructed from a Greenland ice core, *Science*, *270*, 1962–1964, 1995.

Pye, K., *Aeolian Dust and Dust Deposits*, Academic, San Diego, Calif., 1987.

Rea, D. K., The paleoclimatic record provided by eolian deposition in the deep sea: The geologic history of wind, *Rev. Geophys.*, *32*, 159–195, 1994.

Rind, D., Latitudinal temperature gradients and climate change, *J. Geophys. Res.*, *103*, 5943–5971, 1998.

Shea, D., Climatological atlas: 1950–1979, surface air temperature, precipitation, sea level pressure, and sea surface temperature, *Tech. Rep. NCAR/TN-269+STR*, Natl. Cent. for Atmos. Res., Boulder, Colo., 1986.

Steffensen, J. P., The size distribution of microparticles from selected segments of the Greenland Ice Core Project ice core representing different climate periods, *J. Geophys. Res.*, *102*, 26,755–26,763, 1997.

Tegen, I., and I. Fung, Modeling of mineral dust in the atmosphere: Sources, transport, and optical thickness, *J. Geophys. Res.*, *99*, 22,897–22,914, 1994.

Tegen, I., and I. Fung, Contribution to the mineral aerosol load from land surface modification, *J. Geophys. Res.*, *100*, 18,707–18,726, 1995.

Tegen, I., and R. Miller, A GCM study on the interannual variability of soil dust aerosol, *J. Geophys. Res.*, *103*, 25,975–25,995, 1998.

Thompson, L. G., E. Mosley-Thompson, M. Davis, P. N. Lin, T. Yao, M. Dyurgerov, and J. Dai, "Recent warming": Ice core evidence from tropical ice cores with emphasis on Central Asia, *Global Planet. Change*, *7*, 145–156, 1993.

Thompson, L. G., M. Davis, and E. Mosley-Thompson, Glacial records of global climate: A 1500-year tropical ice core record of climate, *Human Ecol.*, *22*, 83–95, 1994.

Thompson, L. G., E. Mosley-Thompson, M. E. Davis, P. N. Lin, J. Dai, and J. F. Bolzan, A 1000 year ice-core record from the Guliya ice cap, China: Its relationship to global climate variability, *Ann. Glaciol.*, *21*, 175–181, 1995*a*.

Thompson, L. G., E. Mosley-Thompson, M. E. Davis, P. Lin, K. A. Henderson, J. Cole-Dai, J. F. Bolzan, and K. Liu, Late glacial stage and Holocene tropical ice core regords from Huascaran, Peru, *Science*, *269*, 46–50, 1995*b*.

Thompson, L. G., T. Yao, M. E. Davis, K. A. Henderson, E. Mosley-Thompson, P. Lin, J. Beer, H. Synal, , J. Cole-Dai, and J. F. Bolzan, Tropical climate instability: The last glacial cycle from a Quinghai-Tibetan ice core, *Science*, *276*, 1821–1825, 1997.

Thompson, L. G., and E. Mosley-Thompson, Microparticle concentration variation linked with climatic change: Evidence from polar ice cores, *Science*, *212*, 812–815, 1981.

Webb, R., C. Rosenzweig, and E. R. Levine, A global data set of particle size properties, *NASA Tech. Rep. NASA TM-4286*, 33 pp., 1991.

Zhang, D., Synoptic-climatic of dust fall in china since historic times, *Sci. Sin., Ser. B*, *27*, 825–836, 1984.

Zobler, L., A world soil file for global climate modeling, *NASA Tech. Rep. NASA TM-87802*, 32 pp., 1986.

D. Rind, NASA Goddard Institute for Space Studies, 2880 Broadway, New York, NY 10025.

I. Tegen, Max-Planck-Institute for Biogeochemistry, P.O. Box 10 01 64, 07701 Jena, Germany. (e-mail: itegen@bgc-jena.mpg.de)

February 26, 1999; revised July 30, 1999; accepted October 19, 1999.

[1]Now at: Max-Planck-Institute for Biogeochemistry, Jena, Germany.

This preprint was prepared with AGU's LaTeX macros v4. File ice formatted January 11, 2000.

Figure 1. Seasonal mixing ratios (in μg dust/kg air) of Asian dust aerosol for the control experiment 0 for the first model layer.

Figure 2. Seasonality of dust at Greenland for the control experiment 0 for deposition (in mg m^{-2} d^{-1}), first layer concentration (in $\mu g/m^3$), dust concentration in precipitation (in mg/kg water), and precipitation (in mm d^{-1}).

Figure 3. Annually and vertically averaged dust mixing ratios for experiments A-D and control experiment 0, together with dust concentrations for only decreased (C-A+0) or increased (D-B+E) global SSTs (in μg dust/kg air).

Figure 4. Zonal mean northward dust transports for experiments A-D and control experiment 0, relative to the total dust content of the atmosphere.

Plate 1. Differences in dust sources (a,b,c), zonal wind speeds (d,e,f), and precipitation (g,h,i) for changes in the latitudinal SST gradient (experiment A minus experiment B) (a,d,g), colder conditions without changes in the temperature gradient (experiment C minus experiment A) (b,e,h), and warmer conditions without changes in the temperature gradient (experiment D minus experiment B) (c,f,i).

Figure 1. Seasonal mixing ratios (in μg dust/kg air) of Asian dust aerosol for the control experiment 0 for the first model layer.

Figure 2. Seasonality of dust at Greenland for the control experiment 0 for deposition (in mg m^{-2} d^{-1}), first layer concentration (in $\mu g/m^3$), dust concentration in precipitation (in mg/kg water), and precipitation (in mm d^{-1}).

Figure 3. Annually and vertically averaged dust mixing ratios for experiments A-D and control experiment 0, together with dust concentrations for only decreased (C-A+0) or increased (D-B+E) global SSTs (in μg dust/kg air).

Figure 4. Zonal mean northward dust transports for experiments A-D and control experiment 0, relative to the total dust content of the atmosphere.

Plate 1. Differences in dust sources (a,b,c), zonal wind speeds (d,e,f), and precipitation (g,h,i) for changes in the latitudinal SST gradient (experiment A minus experiment B) (a,d,g), colder conditions without changes in the temperature gradient (experiment C minus experiment A) (b,e,h), and warmer conditions without changes in the temperature gradient (experiment D minus experiment B) (c,f,i).

Table 1. GCM Results for Annual Average Dust Sources and Dust Concentrations at Greenland

	China Source $mg/m^2/yr$	Central Asia Source $mg/m^2/yr$	Conc. (Layer 1) $\mu g/m^3$	Avg. Mixing Ratio $\mu g/kg$ Air
C (A + colder)	16 ± 7	59 ± 25	0.79 ± 0.14	2.1 ± 0.3
A (increased gradient)	20 ± 8	74 ± 27	0.66 ± 0.17	1.7 ± 0.3
0 (control)	7 ± 4	40 ± 16	0.24 ± 0.07	0.9 ± 0.2
B (decreased gradient)	7 ± 3	36 ± 14	0.13 ± 0.03	0.7 ± 0.1
D (B + warmer)	8 ± 4	23 ± 11	0.09 ± 0.03	0.5 ± 0.1

Table 2. GCM Results for Annual Average Precipitation and Dust Deposition at Greenland

	Depos. Flux $mg/m^2/yr$	Depos. Flux (Wet) $mg/m^2/yr$	Precipitation mm/yr	Conc. (Precip.) $\mu g/kg$ Water
C (A + colder)	52 ± 10	22 ± 5	36 ± 9	490 ± 110
A (increased gradient)	51 ± 12	23 ± 7	57 ± 16	380 ± 90
0 (control)	22 ± 6	14 ± 4	83 ± 22	160 ± 58
B (decreased gradient)	12 ± 3	8 ± 3	98 ± 23	79 ± 22
D (B + warmer)	10 ± 3	7 ± 3	150 ± 30	53 ± 18

Table 3. GCM Results for Dust Sources and Dust Concentrations at Greenland for NH Spring

	China Source $mg/m^2/yr$	Central Asia Source $mg/m^2/Seas$	Conc. (Layer 1) $\mu g/m^3$	Avg Mixing Ratio $\mu g/kg$ Air
C (A + colder)	5.3 ± 2.6	20 ± 8	0.71 ± 0.11	1.6 ± 0.2
A (increased gradient)	$13. \pm 5.$	31 ± 10	1.1 ± 0.24	2.2 ± 0.3
0 (control)	$3.7 \pm 2.$	15 ± 6	0.27 ± 0.09	0.9 ± 0.2
B (decreased gradient)	$3. \pm 1.8$	8 ± 4	0.16 ± 0.04	0.6 ± 0.1
D (B + warmer)	1.8 ± 1	7 ± 3	0.10 ± 0.03	0.5 ± 0.1

Betreff: a letter from yarden oren
Datum: Tue, 11 Jan 2000 08:37:40 IST
Von: "Osnat Birman" <obirman@hotmail.com>
An: knadrow@bgc-jena.mpg.de

Dear Karin
First and eminently a very good and happy new year/decade/century/millennium to you. What are you up to these days? Should we expect to see you back in Israel? (your flags are still out in the field).
Well, back here things look pretty much the same way you left them, a short and warm winter and it will be summer soon. I am still struggling in writing my thesis and searching for a postdoc position, primarily in the US.

Moshe gave me your Ôdiplomarbeit Õ to read and indeed you succeeded in turning you frustration in the field to a nice piece of work, congratulations, really! However, I have a hard time using the computer model itself. Probably I am the one to blame, yet I donÕt find it self explanatory enough to be used simply as is. Is there any manual which may guide me in doing so?
Secondly, I am currently debating in what form to culminate my thesis. I was thinking of using some simulation model, to predict scenarios under different grazing regimes based on data from my small-scale experiment. I was wondering whether the model you created is flexible enough to be modified to do the task. I am interested in simulating patch dynamics in our shrubland in a spatially realistic manner in which patches contract or expand based on soil erosion and deposition. Productivity should be linked to patchiness like in your model via rainfall-runoff relations. Nevertheless, productivity feeds back on itself via bulk seed dispersal with some neighbourhood rules. Any ideas? I appended the general way I view the model (roughly).
If this option is not appropriate I will resort to some simple model I may construct, though I havenÕt figured out how yet. If you have good suggestions, I will be glad to hear.

Simulation model of patchiness,
resource leakage and productivity
Aim: simulate dynamics of patchiness,
resource leakage and productivity on a slope in Sayeret Shaqed based on cell data.

Questions
1. what are the dynamics under ungrazed, lightly and
heavily grazed regimes?
2. what are the dynamics when grazing is restricted
to upper or lower half of the slope?

Iteration process:
0. assign a random
landscape of shrub and crust patches; each patch is assigned a size and productivity.
1. apply grazing to patches
2. set potential productivity per
patch based on former productivity and grazing
3. choose rainfall from
normal distribution
4. apply leakage of runoff and matter between patches
based on cell models;
5. reset productivity based on soil moisture
availability and potential productivity
6. reset patch size based on former
size and soil erosion/deposition

Output:
1. average size of patches
2.
annual water leakage
3. annual productivity
Hope to hear from you soon, Lehitraot

1st Layer Dust Concentration (μg dust/kg air) CONTROL

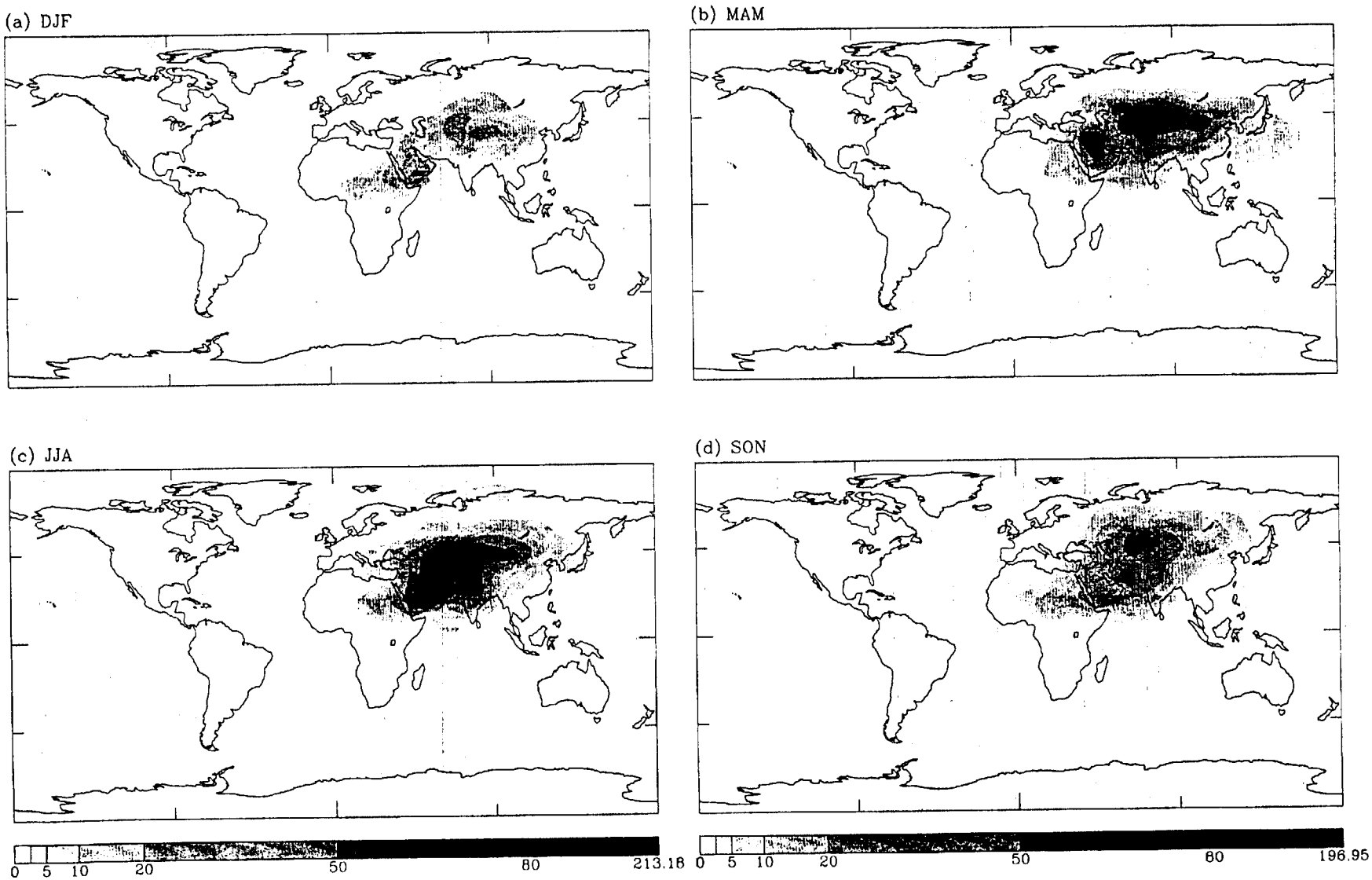

Figure 1

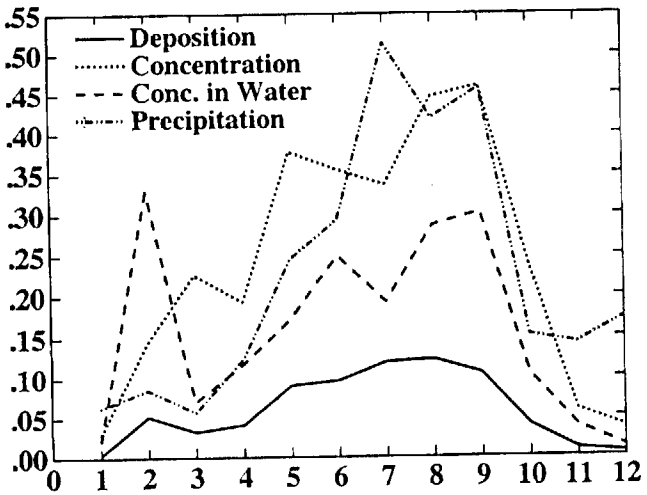
Deposition
Concentration
Conc. in Water
Precipitation
.55
.50
.45
.40
.35
.30
.25
.20
.15
.10
.05
.00
0 1 2 3 4 5 6 7 8 9 10 11 12
Month

Figure 2

Dust Concentration (μg/kg air)

(A) Gradient +9°C

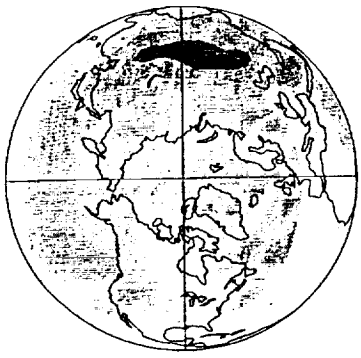

(C−A+0) SST −4°C

(C) Gradient +9°C, SST −4°C

(B) Gradient −9°C

(D−B+0) SST +4°C

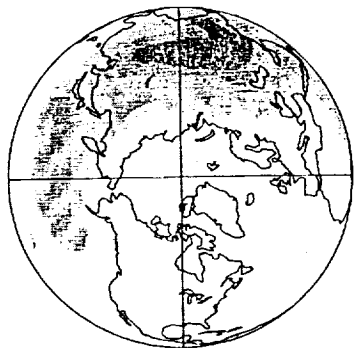

(D) Gradient −9°C, SST +4°C

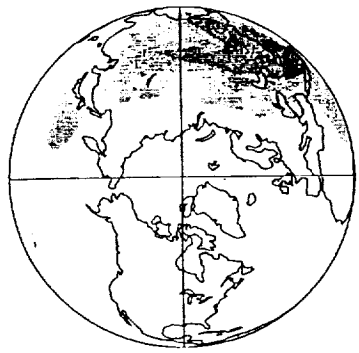

(0) Control − Climatological SST

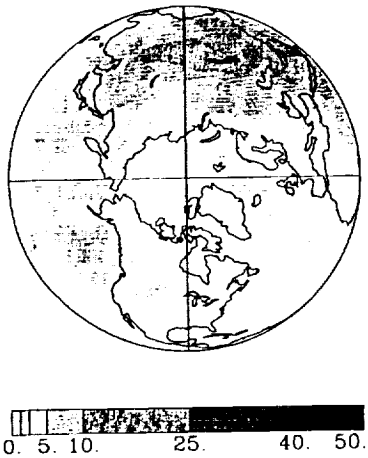

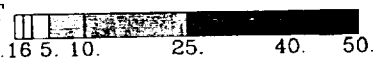

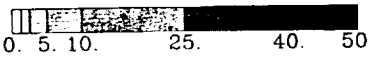

Figure 3

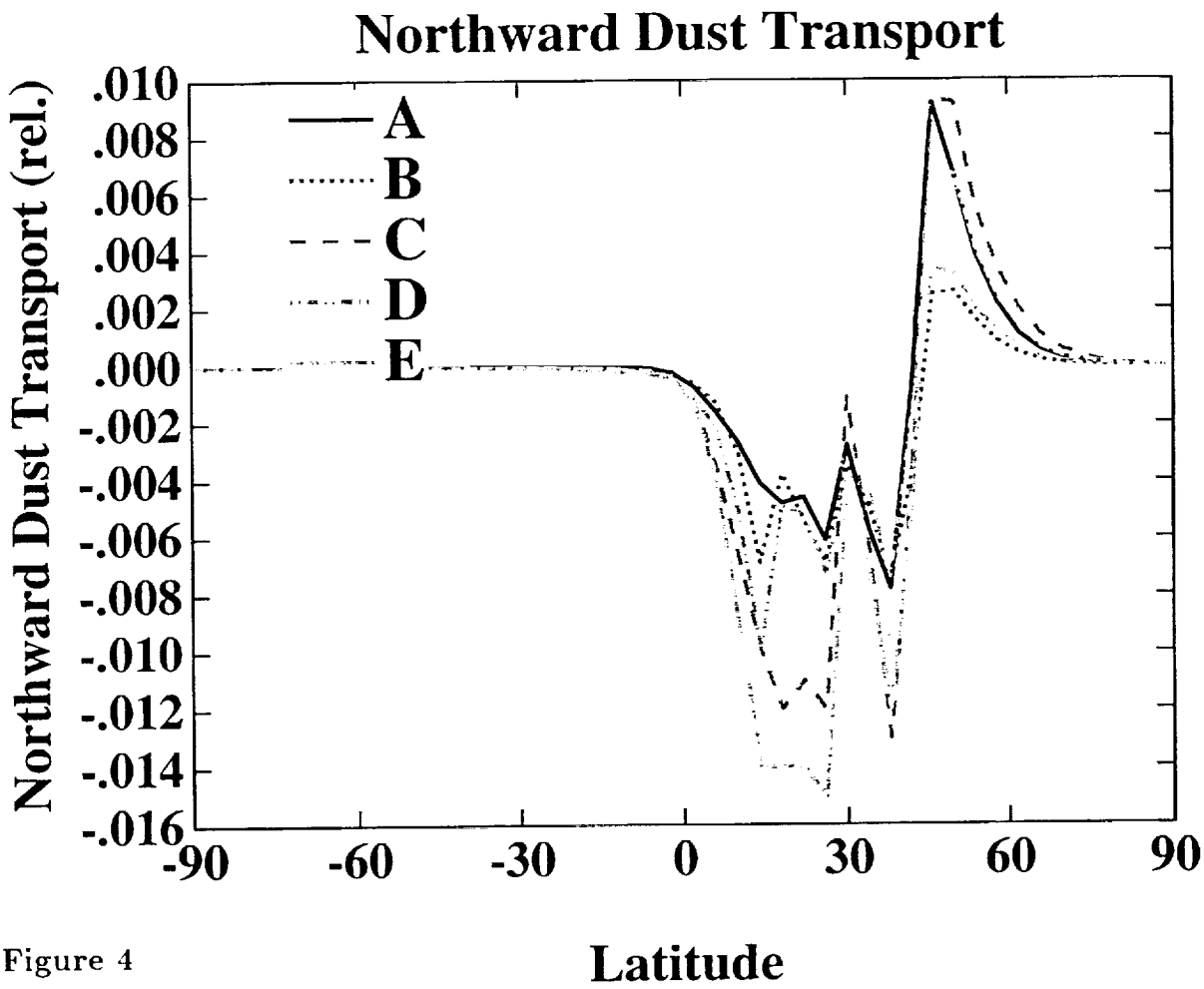
Northward Dust Transport
Northward Dust Transport (rel.)
.010
.008
.006
.004
.002
.000
-.002
-.004
-.006
-.008
-.010
-.012
-.014
-.016
A
B
C
D
E
-90
-60
-30
0
30
60
90
Latitude

Figure 4

Dust Flux ($g/m^2/d$)

(a) Gradient Change (A−B)

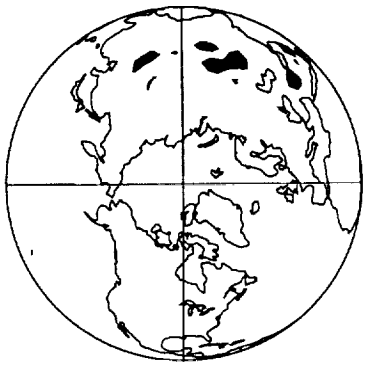

(b) Colder Only (C−A)

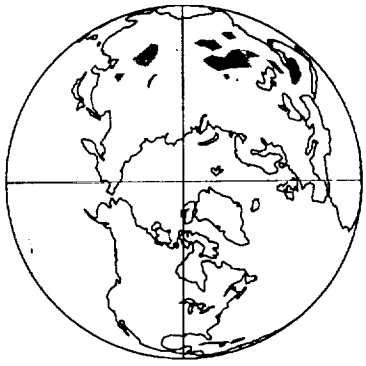

(c) Warmer Only (D−B)

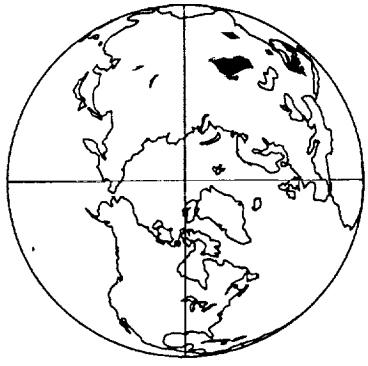

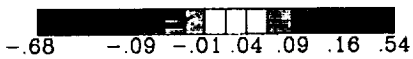

Zonal Surface Wind (m/s)

(d)

(e)

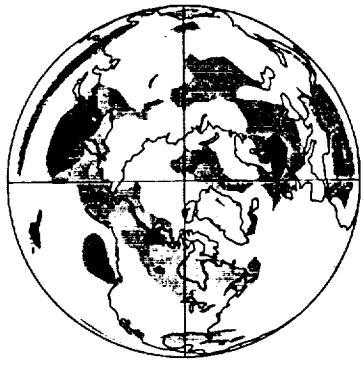

(f)

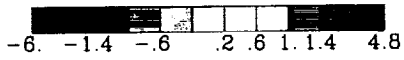

Precipitation (mm/d)

(g)

(h)

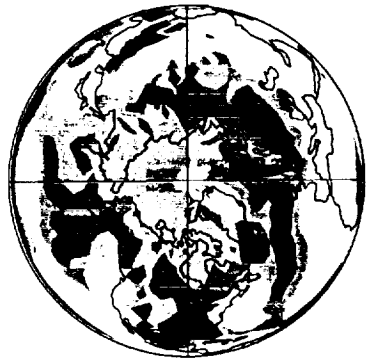

(i)